ISSN 1063-780X, Plasma Physics Reports, 2008, Vol. 34, No. 10, pp. 879–884. © Pleiades Publishing, Ltd., 2008.
Original Russian Text © V.I. Karas', V.I. Golota, O.V. Bolotov, B.B. Kadolin, D.V. Kudin, 2008, published in Fizika Plazmy, 2008, Vol. 34, No. 10, pp. 951–958.

LOW-TEMPERATURE PLASMA

Specific Features of Radiation from a Negative Air Corona Operating in the Trichel-Pulse Mode

V. I. Karas', V. I. Golota, O. V. Bolotov, B. B. Kadolin, and D. V. Kudin

National Science Center Kharkiv Institute of Physics and Technology, National Academy of Sciences of Ukraine, vul. Akademichna 1, Kharkiv, 61108 Ukraine

Received February 6, 2008

Abstract—Experimental studies of spatiotemporal characteristics of radiation from a negative corona operating in the Trichel-pulse mode in the point-to-sphere electrode geometry have revealed two emission zones. In addition to the well-known glow near the point electrode, there is also an anode glow, whose intensity depends substantially on the shape of the anode. It is found that the anode glow is delayed with respect to the beginning of the Trichel pulse by a time that depends on the gap length and gap voltage. The emission spectrum of the anode glow in the wavelength range 300–400 nm is identified as the spectrum of the second positive system of nitrogen (the $C^3\Pi_u$–$B^3\Pi_g$ transition).

PACS numbers: 52.25.Os, 52.80.-s, 52.80.Hc

DOI: 10.1134/S1063780X08100097

1. INTRODUCTION

Studies of corona discharges continue to be a topical problem because a self-consistent model capable of adequately describing the formation and evolution of this type of discharge is still lacking.

It is of special interest to study a negative corona in short gaps at atmospheric pressure. Such a discharge is self-sustained and forms in highly inhomogeneous electric fields characteristic of the point-to-plane electrode geometry in which the discharge is maintained by applying a negative potential to the point electrode. There is a range of discharge voltages in which the discharge current represents a steady-state sequence of the so-called Trichel pulses [1]. An increase in the gap voltage (the other conditions being the same) leads to a decrease in the pulse amplitude and an increase in the pulse repetition rate. At a sufficiently high voltage, the discharge passes into to a diffuse phase [2], in which the current flowing through the discharge gap is constant [3].

As a rule, in constructing a model of a negative corona, the discharge gap is conventionally divided into two regions. A bright ~1-mm-long region adjacent to the corona electrode is referred to as the active zone. This zone is characterized by a high reduced electric field and intense generation of charged particles. The rest of the discharge gap is referred to as the drift zone. The electric field in the drift zone is too low for charged particles to gain an energy necessary for intense ionization; therefore, the current in this region is primarily provided by the drift of negatively charged particles toward the anode. Experimental studies of the spatiotemporal characteristics of radiation from the active zone of a low-pressure corona discharge were reported in [4]. In [5], a model was proposed that described the establishment of a sequence of Trichel pulses in a corona discharge in air after applying a voltage to the discharge gap. Among works devoted to theoretical studies of the mechanism for generating Trichel pulses, it is worth mentioning [6, 7]. In [8], a sequence of Trichel pulses in a low-current negative corona in air was reproduced in numerical simulations. The calculated parameters of individual Trichel pulses turned out to be in good agreement with experimental data, but their repetition rate disagreed with experimental results. Such a discrepancy between experimental data and theoretical models indicates the necessity of continuing experimental studies of negative coronas, especially the processes occurring in the drift zone of the discharge gap.

2. EXPERIMENT

The spatial characteristics of radiation from a negative corona in atmospheric-pressure air were studied by detecting radiation from the cathode and anode regions of the corona with the help of a photomultiplier tube. A block-diagram of the experimental setup is shown in Fig. 1.

As a power supply, we used a stabilized high-voltage source with an output voltage of up to 30 kV. The gap voltage and the average discharge current were measured with an S196 kilovoltmeter and M906 microammeter, respectively. To stabilize the dc high voltage applied to the discharge, high-voltage capacitor *6* with a capacitance of 2200 pF was connected in parallel to the discharge gap. The experiments were performed with the point-to-sphere electrode geometry. The cathode was a 10-mm-long tungsten needle with a

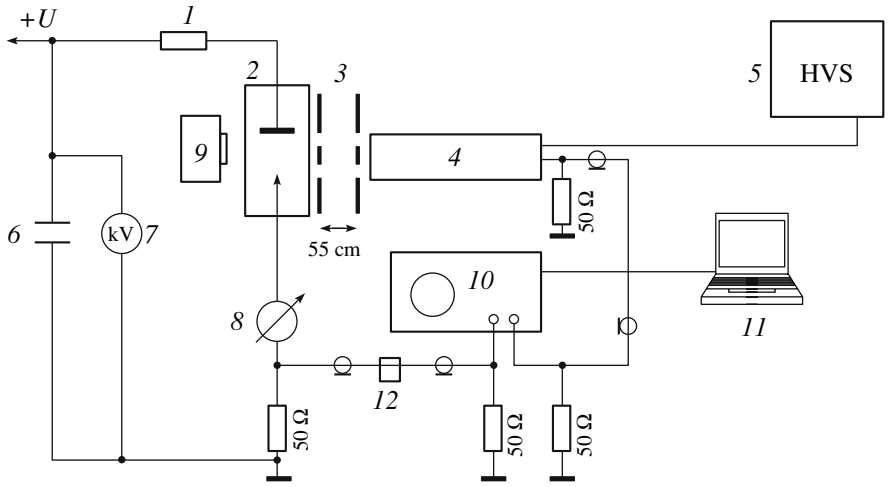

Fig. 1. Block diagram of the experimental setup: (*1*) 130-kΩ ballast resistor, (*2*) discharge cell, (*3*) slit, (*4*) FEU-36 photomultiplier, (*5*) photomultiplier high-voltage supply, (*6*) 2200-pF voltage filtering capacitor, (*7*) S196 kilovoltmeter, (*8*) M906 microammeter; (*9*) Olympus C7070 camera, (*10*) Tektronix TDS210 oscilloscope, (*11*) IBM PC, and (*12*) 38-ns delay line.

tip curvature radius of 20 μm, and the anode was an 8-mm-diameter stainless-steel sphere. The electrode distance was 7, 10, or 15 mm. To provide stable discharge operation, the needle and the sphere underwent special treatment. An indicator of stable discharge operation was a steady-state shape of Trichel pulses, whose formation was determined by the processes occurring in the discharge gap. The steady-state shape and repetition rate of current pulses showed the stability of the discharge conditions under which the Trichel pulses were measured.

The temporal and amplitude characteristics of current pulses were recorded using calibrated current probes, the signals from which were fed to a Tektronix TDS210 oscilloscope with a sampling rate of 1 GHz. The temporal characteristics of radiation from the discharge regions under study were measured using an FEU-36 photomultiplier with a cathode transit time difference (CTTD) of 2 ns and rise time of 3 ns. The spectral sensitivity of FEU-36 is maximum in the wavelength range 300–600 nm. The radiation from the electrode regions was selected using pairs of 20 × 1-mm slits made in two opaque screens spaced a distance of 55 mm. The screens were arranged with respect to the discharge gap and relative one another in such a way that only the regions under study were seen through the slits. A simplified optical scheme of the experiment is shown in Fig. 2.

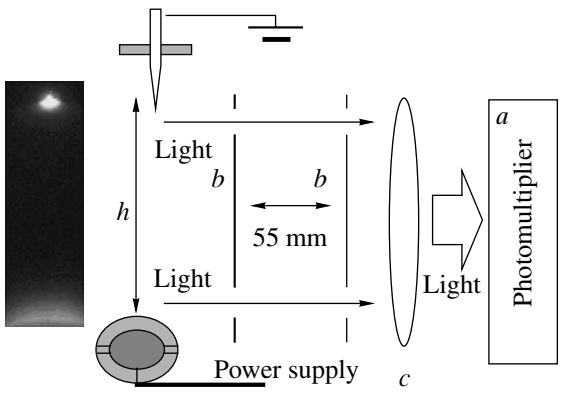

Fig. 2. Photograph of a negative corona and simplified optical scheme of the experiment: (*h*) discharge gap, (*a*) photocathode of the FEU-36 photomultiplier, (*b*) slits, and (*c*) quartz lens.

The discharge current pulses were recorded simultaneously with the signals from the photomultiplier, onto the photocathode of which radiation from both the cathode and anode regions was focused. The slits transmitted radiation only from the regions located at a distance of 1 mm from the electrode surfaces. To compensate for the time delay in the photomultiplier signal due to the finite electron transit time through the photomultiplier and, thereby, to synchronize the current signal with the photomultiplier one, a time-delay line with a time constant of 38 ns was introduced in the circuit measuring the discharge current.

3. EXPERIMENTAL RESULTS

It is found experimentally that, in an atmospheric-pressure corona discharge operating in the Trichel-pulse mode in the point-to-sphere electrode geometry, two light flashes occur during one current pulse. First, a rather short radiation pulse is emitted from the active zone and, then, a glow appears with a certain time delay in the region immediately adjacent to the spherical anode. The glowing region near the anode expands with increasing voltage and can reach the middle of the gap, whereas the cathode glow is localized on the tip of the point electrode. Figure 3 shows typical waveforms of

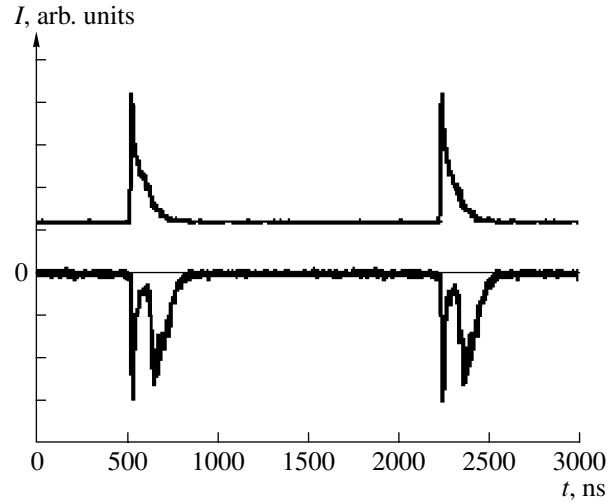

Fig. 3. Typical waveforms of the discharge current (upper curve) and the synchronized photomultiplier signal (lower curve) for a negative corona operating in the Trichel-pulse mode. The gap length is 7 mm, $U = 9.6$ kV, and $I_{av} = 34$ μA.

the discharge current in the Trichel-pulse mode (upper curve) and the synchronized photomultiplier signals (lower curve).

We recorded radiation pulses emitted only from the regions adjacent to the electrodes. It can be seen from Fig. 3 that the discharge current represents a steady-state sequence of pulses with a characteristic duration of ~250 ns and a time interval between pulses of ~2.2 μs. The photomultiplier signals corresponding to the radiation pulses from the cathode and anode regions are separated in time. The radiation pulse from the cathode region begins simultaneously with the current pulse; accordingly, the first spike in the photomultiplier signal corresponds to the light emitted from the cathode region, whereas the second spike corresponds to the light emitted from the anode region. Radiation pulses emitted from the cathode region (~30 ns) are typically much shorter than Trichel pulses (~200 ns), and the duration of radiation pulses emitted from the anode region is on the order of that of Trichel current pulses.

Our experiments have shown that the delay time between by which radiation pulses emitted from the cathode and anode regions depends on the gap length and gap voltage. Figure 4 shows waveforms of the photomultiplier signals corresponding to radiation pulses emitted from discharge gaps of length 7, 10, and 15 mm for different values of the gap voltage U and average discharge current I_{av}.

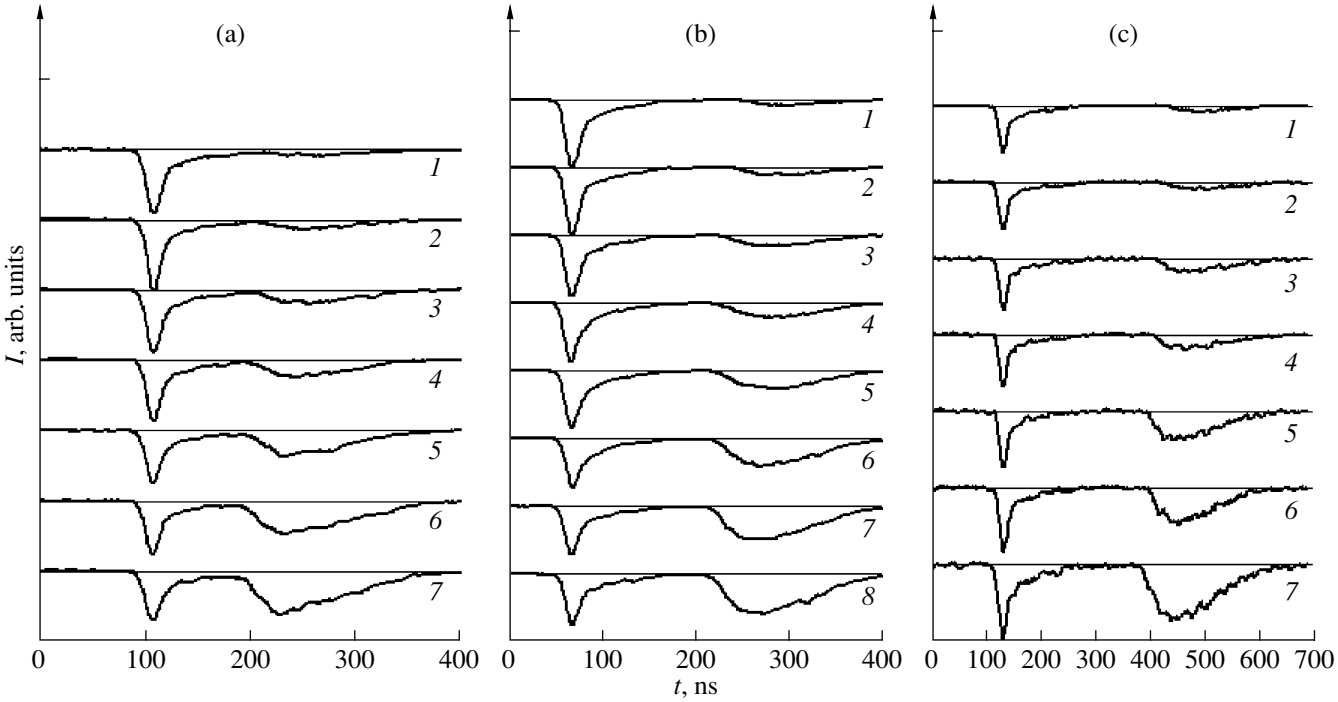

Fig. 4. Waveforms of photomultiplier signals from a negative corona in the point-to-sphere electrode geometry for different gap lengths at different discharge parameters: (a) for 7 mm at (*1*) $U = 7.2$ kV and $I_{av} = 6$ μA, (*2*) $U = 7.8$ kV and $I_{av} = 8$ μA, (*3*) $U = 8.1$ kV and $I_{av} = 12$ μA, (*4*) $U = 8.4$ kV and $I_{av} = 16$ μA, (*5*) $U = 9$ kV and $I_{av} = 20$ μA, (*6*) $U = 9.3$ kV and $I_{av} = 25$ μA, and (*7*) $U = 9.6$ kV and $I_{av} = 34$ μA; (b) for 10 mm at (*1*) $U = 10.1$ kV and $I_{av} = 3$ μA, (*2*) $U = 10.8$ kV and $I_{av} = 5$ μA, (*3*) $U = 11.6$ kV and $I_{av} = 8$ μA, (*4*) $U = 12$ kV and $I_{av} = 10$ μA, (*5*) $U = 12.4$ kV and $I_{av} = 14$ μA, (*6*) $U = 12.8$ kV and $I_{av} = 20$ μA, (*7*) $U = 12.9$ kV and $I_{av} = 25$ μA, and (*8*) $U = 13$ kV and $I_{av} = 31$ μA; and (c) for 15 mm at (*1*) $U = 15$ kV and $I_{av} = 6$ μA, (*2*) $U = 15.3$ kV and $I_{av} = 8$ μA, (*3*) $U = 15.9$ kV and $I_{av} = 12$ μA, (*4*) $U = 16$ kV and $I_{av} = 14$ μA, (*5*) $U = 16.5$ kV and $I_{av} = 20$ μA, (*6*) $U = 16.6$ kV and $I_{av} = 25$ μA, and (*7*) $U = 17$ kV and $I_{av} = 34$ μA.

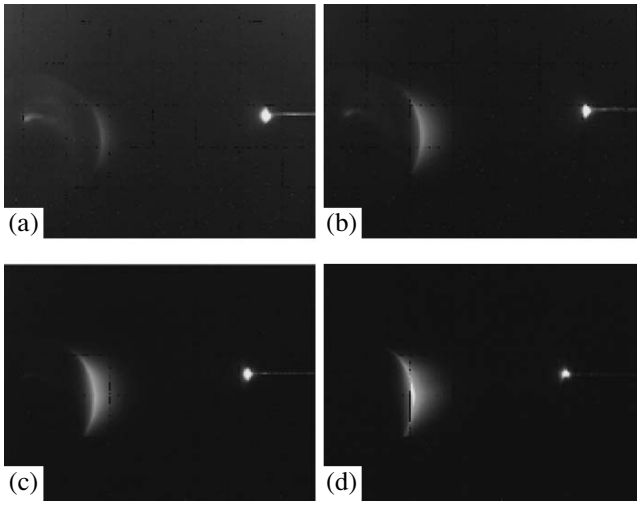

Fig. 5. Images of a negative corona in air in the point-to-sphere geometry with a 10-mm discharge gap: (a) discharge current 5 μA, pulse repetition period 16 μs, and exposure time 120 s; (b) discharge current 10 μA, pulse repetition period 7 μs, and exposure time 60 s; (c) discharge current 18 μA, pulse repetition period 3.1 μs, and exposure time 30 s; and (d) discharge current 31 μA, pulse repetition period 1.6 μs, and exposure time 15 s.

It can be seen that the delay time between the beginnings of radiation pulses emitted from the cathode and anode regions is minimum for a gap length of 7 mm and decreases to 106 ns as the voltage increases to 9.6 kV. The maximum delay time, 320 ns, was observed for the gap length 15 mm and voltage 15 kV.

It is found that the amplitude of radiational pulses emitted from the cathode region increases with increasing amplitude of Trichel pulses and that the amplitude and duration of radiation pulses emitted from the anode region increases monotonically with average discharge current for all of the gaps under study.

The dependence of the amplitude of Trichel pulses on the discharge voltage under our experimental conditions is found to be different for different gap lengths. For gaps of length 7 and 10 mm, the amplitude decreases with increasing voltage, whereas for the 15-mm gap, it increases insignificantly. Such a discrepancy may be related to the use of the point-to-sphere electrode system.

The dependence of the radiation intensity from the cathode and anode regions on the discharge voltage was studied by recording the discharge radiation on a time scale considerably longer that the repetition period of Trichel pulses. Visible light from the entire discharge gap was recorded by an Olympus C7070 digital camera with a fixed objective aperture at different exposures from 0.002 to 120 s.

Figure 5 shows images of a negative air corona in a 10-mm-long point–spherical gap at different discharge currents. The average discharge current was varied from 5 to 32 μA, and the images were taken with different exposures, so that approximately the same number of radiation pulses were recorded on one frame; i.e., the ratio of the exposure to the repetition period of Trichel pulses was kept nearly constant.

It can be seen that, as the amplitude of Trichel pulses decreases, the intensity of radiation pulses emitted from the cathode region decreases, whereas that of radiation pulses emitted from the anode region, as well as the size of the glowing region, increases. This confirms the results of photomultiplier measurements. Indeed, the

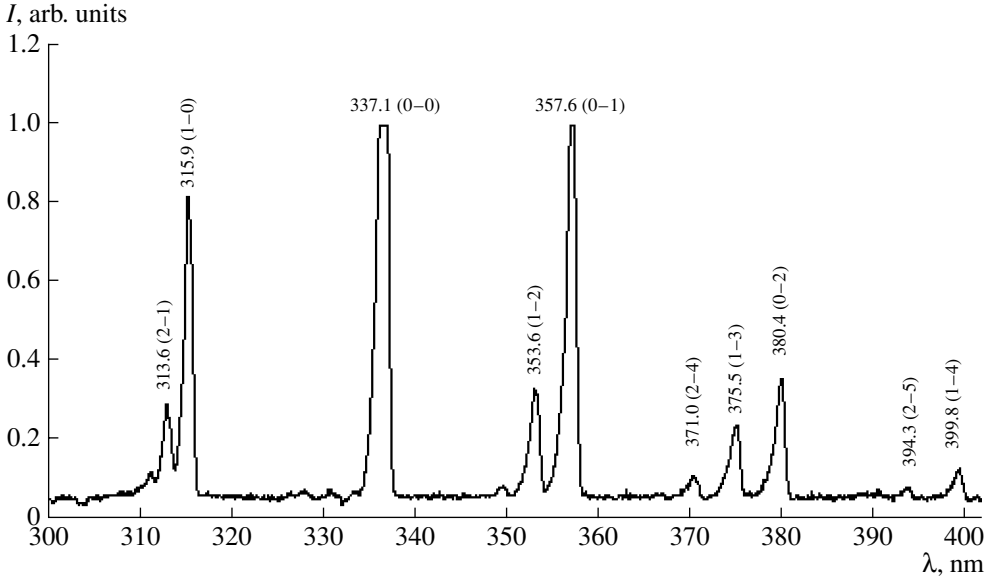

Fig. 6. Emission spectrum from the cathode region of a negative air corona operating in the Trichel-pulse mode in the point-to-sphere electrode geometry. The gap length is $d = 15$ mm, the voltage is 17 kV, and the pulse repetition period is $T = 2.5$ μs.

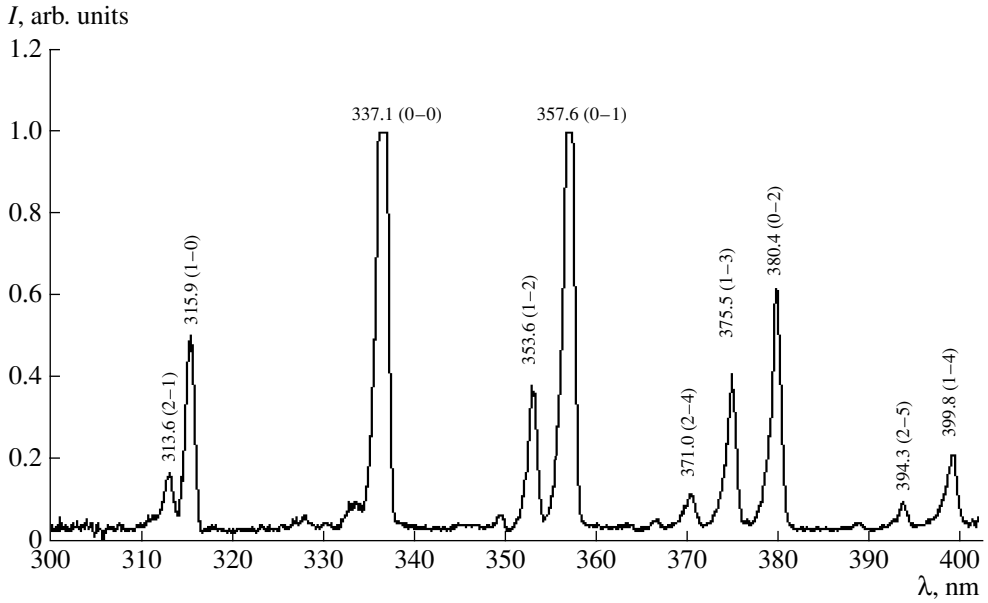

Fig. 7. Emission spectrum from the anode region of a negative air corona operating in the Trichel-pulse mode in the point-to-sphere electrode geometry. The gap length is $d = 15$ mm, the voltage is 17 kV, and the pulse repetition period is $T = 2.5$ μs.

amplitude of the photomultiplier signal corresponding to the radiation pulse from the cathode region (see Fig. 4b) decreases with increasing discharge current, while the amplitude of the second spike increases.

In our experiments, we also measured the emission spectra from the cathode and anode regions in the wavelength range 300–400 nm. The emission spectra were recorded and analyzed using an MDR-12U monochromator, an FEU-106 photomultiplier, a Velleman PCS 500 analog-to-digital converter, an IBM PC, and a PC-Lab2000 software. A comparison of the measured spectra with those presented in [9] indicates that the spectra contain lines of the second positive system of N_2, in particular, those corresponding to the $C^3\Pi_u \longrightarrow B^3\Pi_g$ transition between electronic levels of N_2. In analyzing spectral lines with allowance for vibrational excitation of electronic levels, we used reference data [10] on the rate constants for the emission lines of molecular spectra and molecular and atomic excited states. We calculated the energies of the possible vibrational levels of a nitrogen molecule in the $C^3\Pi_u$ state and ten lower vibrational levels of the $B^3\Pi_g$ state. These energies were then used to calculate all the possible transitions between the $C^3\Pi_u$ and $B^3\Pi_g$ states. The use of reference data on the rate constants and taking into account vibrational excitation of electronic levels made it possible to identify the discharge radiation spectrum in the wavelength range 300–400 nm. Figures 6 and 7 show the radiation spectra from the cathode and anode regions of a negative corona operating in the Trichel-pulse mode.

The identification of the spectrum with the use of reference constants allows us to conclude that the observed spectra are the spectra of the second positive system of molecular nitrogen (the $C^3\Pi_u$–$B^3\Pi_g$ transition). The emission spectrum from the anode region in the wavelength range 300–400 nm is generally similar to that from the cathode region; however, the intensity ratios between lines in these spectra are different.

4. DISCUSSION OF RESULTS

Experimental studies have shown that, in negative coronas operating in the Trichel-pulse mode in the point-to-plane electrode geometry, no light emission from the anode region is observed, in contrast to those in the point-to-sphere geometry at the same discharge parameters (the voltage, average discharge current, and gap length). The difference in the configuration of the electrode system has little effect on the vacuum distribution of the electric field. Nevertheless, in atmospheric-pressure corona discharges produced in the point-to-sphere geometry (at $R \sim d$), the discharge glow can also be observed in the anode region.

The data obtained with a photomultiplier, as well as photographs of a negative corona operating in the Trichel-pulse mode in the point-to-sphere electrode geometry, show that there are two distinct glow regions in the discharge gap. The discharge glow near the point cathode appears simultaneously with the beginning of the current pulse, and its intensity correlates with the amplitude of the Trichel pulse. The radiation pulse from the anode region is delayed with respect to the beginning of the Trichel pulse, and its intensity increases with increasing discharge current. The time delay of the radiation pulse emitted from the anode region with respect to the Trichel pulse increases with increasing

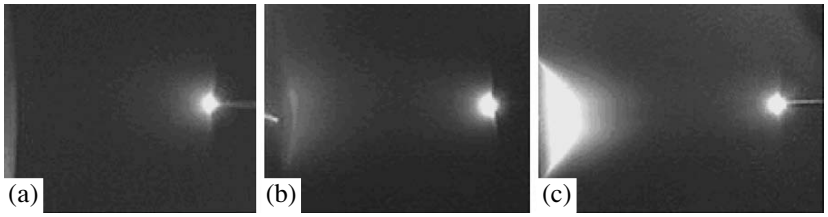

Fig. 8. Images of a negative corona in air for different configurations of the electrode system: (a) point-to-plane geometry at an average discharge current of 43 μA, (b) point-to-truncated cone geometry at an average discharge current of 48 μA, and (c) point-to-sphere geometry at an average discharge current of 48 μA. The plane electrode is a 28-mm-diameter stainless-steel disk, and the diameters of the vertex and base of the truncated cone with a cone angle of 150° are 5 and 34 mm, respectively. The discharge gap is 15 mm. Photographs were taken with an exposure of 120 s.

gap length and decreases with increasing applied voltage. For a given gap voltage and a given gap length, the time delay of the radiation pulse from the anode region with respect to the Trichel pulse is always the same. This indicates that these phenomena are related to one another.

An analysis of the emission spectra from the cathode and anode regions in the wavelength range 300–400 nm indicates that these spectra contain lines of the second positive system of nitrogen (the $C^3\Pi_u$–$B^3\Pi_g$ transition). The spectrum from the anode region in the wavelength range 300–400 nm is generally similar to that from the cathode region; however, the intensity ratios between lines in these spectra are different. This difference can be attributed to different mechanisms by which electrons gain energy in these regions. It can be seen that the population of the upper vibrational levels of the $C^3\Pi_u$ state in the cathode region is greater than that in the anode region, whereas the population of the upper vibrational levels of the $B^3\Pi_g$ state is greater in the anode region.

It should also be noted that the spatial distribution of the discharge glow in a negative air corona operating in the Trichel-pulse mode depends substantially on the shape and dimensions of the anode (see Fig. 8).

A decrease in the cross section of the current channel leads to an increase in the radiation intensity from the anode region.

To reveal the physical mechanism responsible for the interrelation between the formation of Trichel pulses and light emission from the anode region, it is necessary to further investigate the characteristics of radiation emitted from the anode region by using more sensitive detectors.

5. CONCLUSIONS

The experimental studies of the spatiotemporal characteristics of radiation emitted from a negative corona operating in the Trichel-pulse mode in the point-to-sphere electrode geometry have revealed two emission regions. In addition to the well-known glow near the point cathode, there is also an anode glow. The radiation intensity from the anode region is found to depend substantially on the shape of the anode. The emission spectra from the anode and cathode regions in the wavelength range 300–400 nm have been identified as the emission spectra of the second positive system of nitrogen (the $C^3\Pi_u$–$B^3\Pi_g$ transition). It is found that the emission spectrum from the anode region in the wavelength range 300–400 nm is generally similar to that from the cathode region; however, the intensity ratios between lines in these spectra are different.

It is shown experimentally that the glow region near the anode arises as a result of the processes occurring near the cathode, because at the same gap voltage and gap length, it always appears with the same time delay with respect to the Trichel pulse.

ACKNOWLEDGMENTS

This work was supported in part by the Science and Technology Center in Ukraine (project no. R287).

REFERENCES

1. G. W. Trichel, Phys. Rev **54**, 1078 (1938).
2. Yu. S. Akishev, M. E. Grushin, V. B. Karal'nik, and N. I. Trushkin, Fiz. Plazmy **27**, 550 (2001) [Plasma Phys. Rep. **27**, 520 (2001)].
3. Yu. P. Raizer, *Gas Discharge Physics* (Nauka, Moscow, 1987; Springer-Verlag, Berlin, 1991).
4. R. S. Zentner, Z. Angew. Phys. **29**, 294 (1970).
5. Yu. S. Akishev, M. E. Grushin, I. V. Kochetov, et al., Fiz. Plazmy **25**, 998 (1999) [Plasma Phys. Rep. **25**, 922 (1999)].
6. R. Morrow, Phys. Rev. A **32**, 1799 (1985).
7. R. Morrow, Phys. Rev. A **32**, 3821 (1985).
8. A. P. Napartovich, Yu. S. Akishev, A. A. Deryugin, et al., J. Phys. D **30**, 2726 (1997).
9. R. W. B. Pearse and A. G. Gaydon, *The Identification of Molecular Spectra* (Chapman & Hall, London, 1941; Inostrannaya Literatura, Moscow, 1949).
10. B. M. Smirnov and A. S. Yatsenko, in *Plazma Chemistry*, Ed. by B. M. Smirnov (Énergoatomizdat, Moscow, 1989), Vol. 15, p. 93 [in Russian].

Translated by N.F. Larionova